Volume 1 | Number 1 | Jan 2013 | Pages 1–100

PCCP

Physical Chemistry Chemical Physics
www.rsc.org/pccp

ROYAL SOCIETY
OF CHEMISTRY

ROYAL SOCIETY
OF CHEMISTRY

www.rsc.org/pccp

Spontaneously electrical solids in a new light

Jérôme Lasne[a†], Alexander Rosu-Finsen[a], Andrew Cassidy[b], Martin R.S. McCoustra[a], David Field[b*]

[a] Institute of Chemical Sciences, Heriot-Watt University, Riccarton, EH14 4AS Edinburgh, United Kingdom.
[b] ISA, Department of Physics and Astronomy, Aarhus University, DK-8000 Aarhus C, Denmark
5 [†]Current address: Laboratoire Interuniversitaire des Systèmes Atmosphériques (LISA), CNRS UMR 7583, Université Paris-Est Créteil, Université Paris Diderot, Faculté des Sciences et Technologie, 61 avenue du Général de Gaulle, 94010 Créteil Cedex, France
*Author to whom correspondence should be addressed: dfield@phys.au.dk

10 Reflection-absorption infrared spectroscopy (RAIRS) of nitrous oxide (N_2O) thin films is shown to provide an independent means of observing the spontelectric state, the first new structural phase of matter, with unique electrical properties, to have emerged in decades. The presence of a spontaneous and powerful static electric field within the film, the defining characteristic of spontelectrics, is demonstrated through observations of longitudinal-transverse optical (LO-TO) splitting in RAIR spectra, using an analysis based on the vibrational Stark effect. In particular the dependence of the LO-TO splitting on the film deposition temperature may be wholly 15 attributed to the known temperature dependence of the spontelectric field.

1. Introduction

20 Spontaneously electrical solids, so-called 'spontelectrics',[1,2,3,4,5,6,7] represent a new electrical phase of the solid state. The characteristic property of spontelectric materials is that they exhibit an electric field within the bulk of the solid, without any outside intervention. These fields are spontaneous, created 25 without any external stimulus, such as an applied electric field; hence the term 'spontelectric', an illision of 'spontaneously electrical'. Essentially, it has been found that if one condenses a gas onto a solid surface, a film may be formed which spontaneously exhibits a static electric field. Numerous data, 30 outlined in [1], and its corresponding analysis, point to dipole orientation as the origin of the spontaneous polarization giving rise to these electric fields.

The molecular materials of which spontelectric films are 35 composed have one thing in common: the individual species must possess a permanent dipole moment. Other than that, the species are very diverse, ranging over simple hydrocarbons, halocarbons, alcohols, organic formates, benzene derivatives and such simple inorganics as nitrous oxide (N_2O), the latter being 40 the subject of the current work. Films of material may contain electric fields which can exceed 10^8 V m^{-1}, noting that the breakdown fields of solids typically lie between 10^8 to 10^9 V m^{-1}.

Spontelectrics exhibit polarization through dipole orientation in 45 the material, where this polarization is the origin of the electric field mentioned above. The salient properties of spontelectrics, described in detail in [1] and further in [6,7], are that (i) the spontelectric field is lower for higher deposition temperatures (but see [5]), (ii) the nature of the substrate has no bearing on the 50 strength of the bulk spontelectric field, (iii) the spontelectric field depends on both the nature of the material which is deposited and on the temperature at which the film is deposited, (iv) at greater than a certain temperature of deposition, no spontelectric effect can be observed, (v) there exists a critical temperature, termed 55 the Curie point by analogy with ferromagnetism, at which films depolarize and the spontelectric field disappears.

The spontelectric phase is unique in the physics of solids and shows non-linear and non-local characteristics, making it quite 60 distinct from any other known phase, such as the ferroelectric phase of matter. It also appears to be very widespread, much more so than the ferroelectric phase. As such, it is of considerable value to furnish independent evidence for the existence of this new phase, over and above that already described in the 65 literature. The latter has been limited to the use of a direct electron repulsion technique. The object of the current work is to report just such an independent verification of the spontelectric phenomenon. This is performed using infrared (IR) spectroscopy.

70 The essential physics of the current work is as follows. The spontelectric field results in a vibrational Stark effect in the solid causing a shift in characteristic vibrational frequencies.[8,9,10,11] Since the strength of the spontelectric field depends strongly on the temperature of deposition of the film of material, there is a 75 corresponding temperature dependence of the vibrational frequencies measured using RAIRS. Based upon a model for the spontelectric effect1, we show in section 3 that the apparent LO-TO splitting in solid N_2O has a significant contribution from the Stark effect arising from the spontelectric field. We find here that 80 at a deposition temperature of 48 K, for example, the Stark effect contributes ~30% of the total measured splitting. However the observed temperature dependence of LO-TO splitting is attributed wholly to the dependence of the spontelectric field on the film deposition temperature. An analytical description of this 85 is given in section 3.

For simplicity, we refer throughout to the observed spectral

splitting in N_2O as LO-TO splitting, whilst recognizing that the absolute value of the splitting arises through a combination of the intrinsically different vibrations associated with LO and TO modes and, at the level of approximation adopted here, an
5 independent contribution due to the vibrational Stark effect.

In the current work, spontelectric films are interrogated using RAIRS with a grazing infrared beam, such that the incident electric field of the beam has components both parallel and
10 perpendicular to the film normal. Relative to the incident beam wavelength, the film can be considered infinite in the plane of the film and only transverse optical (TO) phonons can be excited in this plane. If however the thickness of the film is comparable to the wavelength of the incident beam, the boundary conditions
15 allow for the excitation of longitudinal optical (LO) phonons along the normal axis. This is known as the Berreman effect[12], and has been studied extensively in non-ionic films, including N_2O.[13,14,15] Longitudinal phonons resonate at higher frequencies, in general because of the induced field associated with
20 longitudinal waves passing through a dipolar medium. Thus, LO-TO splitting occurs for normal vibrational modes when a grazing incident beam interrogates a thin film. Henceforth ν_L and ν_T represent the frequencies for the LO and TO phonons respectively and $\Delta\nu = \nu_L\text{-}\nu_T$ represents the value of the splitting.
25 Here we propose, as indicated above, that the force field for vibrational modes normal to the surface is modified by the vibrational Stark effect[16,17,18,19] through the presence of the spontelectric field. We show that the presence of the static spontelectric field, oriented along the surface normal, and whose
30 values were obtained in previous work1, can reproduce RAIRS measurements of both the LO-TO splitting, relative to ν_T, and its temperature dependence.

2. Experimental method and results

2.1. The experimental method

RAIRS experiments were performed in an ultrahigh vacuum
40 system, described elsewhere.[20,21] The substrate, an oxygen-free high conductivity copper block coated with a 300 nm amorphous silica layer,[22] is mounted on the end of a closed-cycle helium cryostat, reaching a base temperature of 18 K, measured with a KP-type thermocouple connected to an IJ-6 temperature
45 controller (IJ Instruments). The central chamber is equipped with a line-of-sight quadrupole mass spectrometer (QMS, Hiden Analytical) and a Fourier-transform infrared spectrometer (Varian 670-IR) used in reflection-absorption mode, at a grazing incidence of 75° with respect to the normal to the substrate. After
50 reflection from the sample, the IR beam is focused into a liquid nitrogen cooled HgCdTe detector. The RAIR spectra presented here result from the co-addition of 512 spectra recorded at 1 cm^{-1} resolution.

55 Films are deposited by background dosing of N_2O gas (Sigma-

Aldrich, purity ≥ 99.998%) onto the substrate at a rate of 0.14 ML s^{-1}. Thicknesses of N_2O films in monolayers (ML) were determined (±20%) through temperature-programmed desorption experiments, performed by applying a heating ramp of 0.6 K s^{-1}
60 from the deposition temperature, with desorbed species detected using the QMS. Exposures are expressed in units of Langmuir (1 $L = 10^{-6}$ Torr s) where an ionisation coefficient of N_2O molecules in the ion gauge of 1.2 is taken into account.[23]

2.2. Results

Figure 1 shows a typical RAIR spectrum for a N_2O multilayer. Spectral fitting of the LO and TO bands of the NN stretching mode (νNN) in RAIR spectra of solid N_2O films was performed
70 with Gaussian functions using the Igor Pro software. The fits allow the frequencies to be quoted to ±0.1 cm^{-1} for the longitudinal mode and ±0.2 cm^{-1} for the transverse mode, which shows broader features (see Fig. 1). The quoted uncertainties correspond to the maximum variation that can be applied to the
75 central value of the fitted peak whilst maintaining a match between the experimental spectrum and the fitted curve.

The choice of substrate for these experiments was determined by the metal surface selection rule, which dictates that TO modes
80 are silent on a metal surface. This may be seen in the inset to Figure 1, where the TO mode is absent on a flat, clean Cu substrate. The presence of the silica layer coating, on the copper, relaxes this selection rule and allows the observation of both LO and TO modes in solid N_2O on silica, while retaining the
85 enhanced sensitivity associated with RAIR spectroscopy.
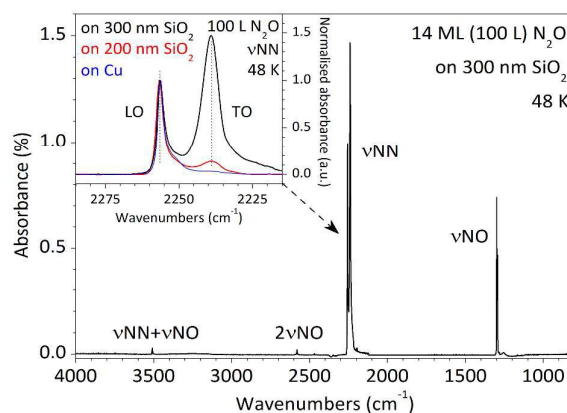
Figure 1. RAIR spectrum of a 100 L (14 ML) N_2O film deposited at 48
90 K on a copper plate coated with 300 nm silica. The inset shows the νNN region[24,25] of the RAIR spectra of 100 L N_2O films deposited on bare copper (blue), on copper coated with a 200 nm (red) or 300 nm (black) amorphous silica layer at 48 K. The intensity of each spectrum has been normalized to that of its LO mode. Dotted lines highlight the positions of
95 the LO and TO modes. All spectra were recorded at 48 K.

The inset to Figure 1 also shows that, at a fixed temperature, the LO and TO modes are located, within experimental uncertainty, at the same frequency on all substrates used. Their relative

intensities however vary with silica layer thickness, with more intense TO relative to LO for thicker layers. The characteristics of the spontelectric effect do not depend on the nature of the substrate on which the films are deposited1. Thus the quantitative use of the RAIRS data remains valid in conjunction with models, described below, based on surface potential measurements performed for example on gold or solid Xe.

Figure 2 shows the vNN band of 14 ML N_2O films, deposited between 48 and 66 K, on 300 nm silica. The inset presents the RAIR spectrum of the film deposited at 48 K (open symbols) and the Gaussians used to fit the LO and TO modes (full lines) for frequency determination. One can see that increasing the deposition temperature red-shifts the LO mode, whilst the TO mode is blue-shifted.
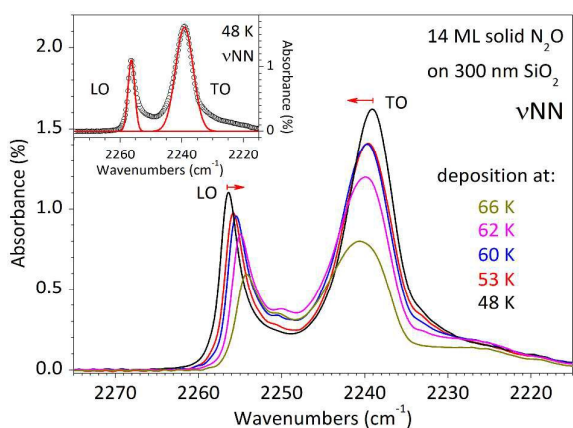
Figure 2. RAIR spectra showing the vNN band of 14 ML N_2O films deposited at 48, 53, 60, 62 and 66 K on 300 nm silica. The arrows highlight the shift of the LO and TO modes with increasing deposition temperature of the films. The inset presents the RAIR spectrum of the film deposited at 48 K (open symbols) and the Gaussian fits to the LO and TO modes (full lines). All spectra were recorded at the respective deposition temperatures.
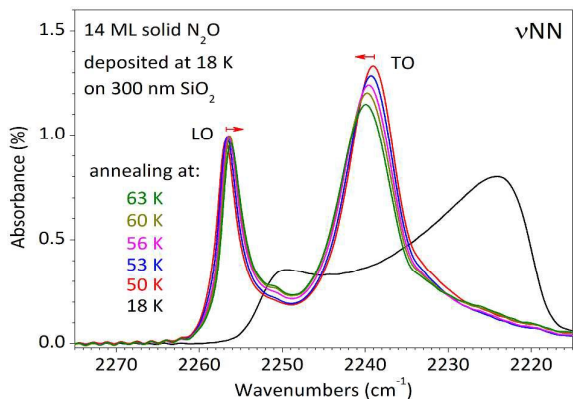
Figure 3. RAIR spectra collected at 18 K showing the vNN band of a 14 ML N_2O film deposited at 18 K on 300 nm silica (broad spectrum) and after annealing to 50, 53, 56, 60 and 63 K. The arrows highlight the shift of the LO and TO modes.

Figure 3 shows RAIR spectra of the vNN band of a 14 ML N_2O film deposited at 18 K on 300 nm silica and after progressive annealing to 50, 53, 56, 60 and 63 K. During the annealing process, the temperature is slowly raised to the indicated value, and left for 5 minutes, noting that longer annealing times give similar results. The film is then cooled down to base temperature (18 K) to record a RAIR spectrum. Annealing the film slightly red-shifts the LO mode, and blue-shifts the TO mode; this is qualitatively what is seen when increasing the deposition temperature (Figure 2), although the shifts are smaller during annealing. Figure 4 shows data for the vNN LO (stars) and TO (circles) modes of 14 ML N_2O films, deposited on 300 nm silica, as a function of both deposition and annealing temperature, as deduced from fits to experimental data shown in Figures 2 and 3.
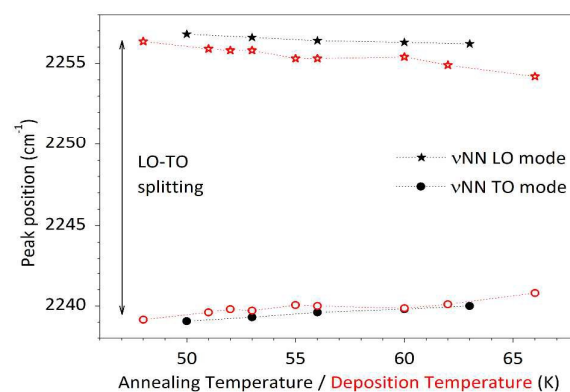
Figure 4. Peak position of the vNN LO (stars) and TO (circles) modes of 14 ML N_2O films deposited on 300 nm silica, as a function of deposition and annealing temperature, deduced from fits to experimental data. Full symbols correspond to the annealing of the 14 ML N_2O film deposited at 18 K and subsequently annealed to the temperatures shown; open symbols correspond to 14 ML N_2O films deposited at the temperatures shown. The lines are a guide for the eye. Errors in frequencies are ±0.1 and ±0.2 cm^{-1} for LO and TO, respectively. Data are collated in Table 1, section 3.3.
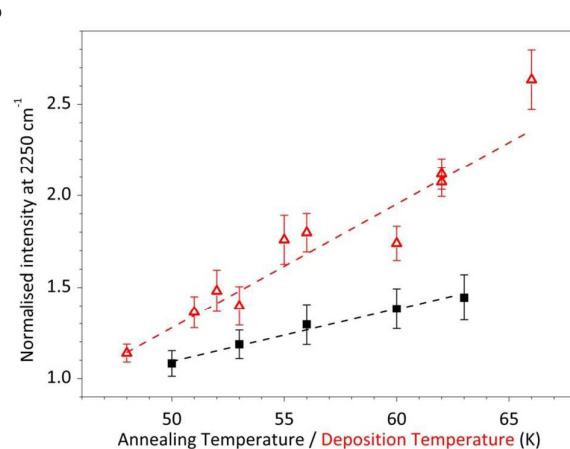
Figure 5. Intensity measured at 2250 cm^{-1} in the RAIR spectra and normalized by the total area of the vNN band for each spectrum, as a

function of temperature. Full symbols correspond to the annealing process of the 14 ML N₂O film deposited at 18 K; open symbols correspond to 14 ML N₂O films deposited at various temperatures. The dotted lines result from a linear fit of the data but are only presented here to guide the eye.

It has been found that LO-TO splitting can be observed at lower temperature than in the data shown here, but with strong inhomogeneous spectral broadening due to the amorphous nature of the films below 48 K. Characteristic low temperature data are shown in Figure 3 for 18 K. Sharp RAIRS data can be obtained on films only at deposition temperatures ≥ 48 K and the present study is limited to a discussion of this temperature regime only.

We may also use the variation of the inhomogeneous broadening of LO and TO bands, with annealing and deposition temperature, as a qualitative indication of the degree of dipole orientation in the film. Figure 5 shows a measurement of the inhomogeneous broadening of the vNN band for both annealing and deposition temperatures. The degree of broadening is estimated by measuring the intensity of the RAIR spectrum at 2250 cm^{-1}, the average frequency of the LO and TO modes, and normalizing by the integrated area of the band. This allows comparison between different experiments and yields the ordinate in Figure 5. This figure illustrates that the increase in inhomogeneous broadening with deposition temperature is ~50% larger than with annealing temperature. Insofar as inhomogeneous broadening is a measure of the range of environments in which any component species finds itself, the greater the inhomogeneous broadening the less the dipole orientation. Results in Figure 5 are therefore consistent with data, recorded in [1], which show that the drop in dipole orientation is greater with an increasing deposition temperature, as opposed to an increasing annealing temperature, over the same temperature range.

3. A theoretical model for the spontelectric Stark effect

The sharpness and well-defined splitting of the vNN peaks at and above 48 K, just referred to, indicate that these spectra relate to films with a significant degree of structural order. Viewing the film as a partially disordered crystal, optical phonons can be recognized, which propagate molecular vibrations throughout the film. It is helpful to envisage transverse optical (TO) phonons as vibrations which arise while preserving the structural form of the film, as sketched on Figure 6. The internal electronic structure of the individual molecules (the two mesomeric forms of N₂O molecules are depicted in Figure 6), influenced by electrostatic effects from neighbouring molecules, is responsible for TO modes. In this mode, there are no relative motions of the molecular species to induce additional electrostatic interactions, and hence they lie at frequencies close to the normal modes of gas-phase molecules. The vibrations of longitudinal optical (LO) phonons, by contrast, involve physical displacement of the molecules, such that molecular dipoles move relative to one another. This relative movement intrinsically stiffens the

potential describing the LO vibrations. Thus LO vibrations are shifted to higher energies (*i.e.* higher frequencies) compared with TO.
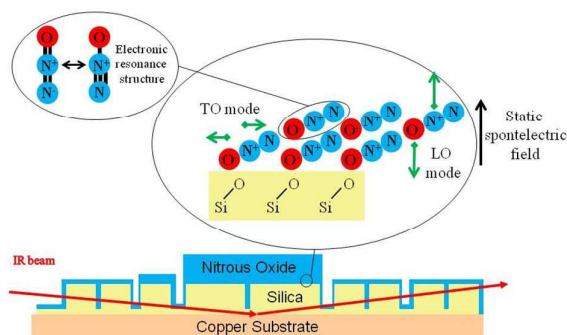
Figure 6. Schematic representation of the experimental geometry showing a multilayered film of N₂O covering a SiO₂ surface; the binding of N₂O to silica through the oxygen end is shown in Ref. [26]. The displacement of charges induced by phonon propagation in the film is shown with green arrows. TO modes do not imply any change in the position of the centre of mass of N₂O molecules, whereas LO modes do. Hence, TO modes do not trigger any relative motion of N₂O molecules but LO modes cause molecular dipoles to oscillate against each other. Both types of modes are activated by the light source in a grazing angle geometry. The static spontaneous electric field is aligned perpendicular to the silica substrate. The combination of silica surfaces parallel and perpendicular to the copper substrate allows modes forbidden by the metal surface selection rule to be observed.

We now seek to relate the variation of the frequencies of LO and TO bands, with deposition temperature, to the properties of spontelectrics. As mentioned in the introduction, we set out to test whether the decrease of the LO-TO splitting, with increasing deposition temperature, can be attributed to the corresponding decrease of the spontelectric field with increasing temperature. An analytical model has been developed elsewhere, which describes the variation of the spontelectric field with temperature.[1] The model is briefly reviewed below. This model is then coupled to the linear vibrational Stark effect. Expressions are developed which explicitly yield the variation of LO and TO frequencies with temperature of deposition. On substitution of suitable spontelectric parameters, described in section 3.2 and evaluated in section 3.4.3, these expressions are found to give a satisfactory description of our experimental observations.

In section 3.1, we first consider possible causes for the temperature variation of the LO-TO splitting, other than the temperature variation of the spontelectric field just mentioned. In section 3.2, we outline the model for the spontelectric phase. In section 3.3, we derive, from experimental data, the relative contributions, of the intrinsic LO-TO effect and the spontelectric Stark effect, to the values of these LO-TO splittings, as a function of deposition temperature. Section 3.4 sets out the model for the temperature dependence of the LO and TO spectral features based upon vibrational Stark tuning and the spontelectric model. Section 3.5 provides a comparison between experimental

results for the variation of the LO-TO splitting with deposition temperature and those computed from the spontelectric Stark effect.

3.1. Other contributions to the variation with deposition temperature of the LO-TO splitting in solid N_2O

In sections 3.1.1 and 3.1.2 below, we consider two possible contributions, other than spontelectric Stark tuning, to the observed reduction of LO-TO splitting with increasing temperature of deposition and of annealing of films.

3.1.1. The effect of thermal expansion with increasing deposition temperature

At higher temperature, the material, being less dense, is composed of molecules sitting at a greater average distance apart and thus more weakly interacting. Since the LO frequency is associated with molecular dipoles effectively rubbing against each other, the LO-TO splitting should therefore decrease with decreasing density.

This effect is described by equation 4 of [**Error! Bookmark not defined.**], which relates the dipole moment derivative associated with the relevant vibration, $\partial\mu/\partial Q$, where Q is the normal coordinate, to the density of the solid material and the LO-TO splitting. Rewriting this equation, we find that the density of material, N, in molecules cm^{-3}, is given by

$$N = 2.037 \times 10^{17} \left(\nu_L^2 - \nu_T^2\right)/(\partial\mu/\partial Q)^2 \qquad (1)$$

where values of ν_L, the LO frequency and ν_T, the TO frequency, at 48 K are 2256.35±0.1 cm^{-1} and 2239.15 ±0.2 cm^{-1} respectively, and $\partial\mu/\partial Q = 0.292$ for vNN in N_2O, the latter figure in SI units. In passing we note that Equation (1) yields N = 1.848 × 10^{22} molecules cm^{-3} which corresponds to a density of 1.36 g cm^{-3}, close to a reported value of 1.35 g cm^{-3} of bulk solid N_2O, at an unrecorded temperature (Encyclopedia Astronautica). At all events, Equation (1) shows that $\Delta\nu \propto N/(\nu_L + \nu_T)$. Thus Equation (1) quantifies what we had already surmised, that thermal expansion associated with a higher deposition temperature or annealing of the film, and therefore a lower density, could be the origin of a decrease in $\Delta\nu$, or of a proportion of the decrease.

We now make the assumption that the mean of ν_L and ν_T is independent of the density of oscillators in the solid, N. Writing the LO-TO splitting as $\Delta\nu$ and inserting the relevant values into (1), we find N = 1.074 × 10^{21} $\Delta\nu$. Thus that $\partial N/\partial\Delta\nu = 1.074 \times 10^{21}$ cm^{-3} per cm^{-1} of increase of $\Delta\nu$. Using experimental deposition data in Figure 4 and Table 1 between 48 and 51 K as an example, $d\Delta\nu/dT = -0.3$ cm^{-1} K^{-1}. This implies that dN/dT, the thermal expansion coefficient of solid N_2O, takes the value $dN/d\Delta\nu.d\Delta\nu/dT = -3.22 \times 10^{20}$ cm^{-3} K^{-1}. This states that there are 3.22 × 10^{20} fewer molecules of N_2O cm^{-3} for every degree K increase in temperature. This is equivalent to a volume expansion coefficient of 0.017 K^{-1}, given that there are 1.848 × 10^{22}

molecules cm^{-3} in solid N_2O at 48 K, as recorded above.

However typical low temperature volume expansion coefficients for molecular materials lie between 10^{-5} and 10^{-6} K^{-1}, showing therefore that thermal expansion cannot be the origin of the decrease in $\Delta\nu$ with temperature observed here. Thus thermal expansion makes no significant contribution to the variation of $\Delta\nu$ with deposition temperature.

3.1.2. Artefacts due to changes in film thickness with temperature of deposition

Film thickness and LO-TO splitting are correlated. To demonstrate this, control experiments (not shown) were performed in which spectra were recorded as a function of increasing thickness of N_2O at 50 K. For example, a comparison of a 7 ML film with one of 14 ML shows that the LO mode is redshifted by -0.3 cm^{-1} and the TO mode is blueshifted by 0.2 cm^{-1}, in the 7 ML film compared with the 14 ML film. Therefore any decrease in true film thickness at higher deposition temperatures could account for some proportion of the observed decrease in $\Delta\nu$.

We now must consider whether there is any correlation between film thickness and temperature of deposition. It was found that the intensities of the vNN LO and TO modes were lower by a factor of ~2 in spectra recorded after deposition at 66 K, compared to deposition at 48 K. Given that the intensity of the vNN LO and TO modes is proportional to the film thickness, the control experiments described above inform us that such a corresponding decrease in thickness of a factor of two might account for a contraction of the LO-TO splitting by roughly 0.5 cm^{-1}. This may be compared with the contraction observed in deposition experiments, which is 3.8 cm^{-1} between 48 and 66 K. In passing we note that the inferred decrease in film thickness between 48 and 66 K is likely due to the decrease of the sticking coefficient of N_2O molecules, when the temperature of the silica substrate is raised to 66 K, close to the sublimation point. Thus the apparent same dose of gas gives rise to a thinner film. Given that any effect on $\Delta\nu$ upon growth of a thinner film is small, we have chosen to ignore the influence of film thickness in our subsequent analysis of experimental data for $\Delta\nu$ vs deposition temperature.

3.2. A brief resume of the model for the spontelectric effect

We now return to the central theme of this section: the spontelectric effect as the origin of a significant fraction of the observed LO-TO splitting and of its variation with deposition temperature. Recollecting that the spontelectric effect is believed to arise through dipole orientation within the bulk of the solid film, data may be interpreted in terms of a decrease in the orientation of dipoles in N_2O films, with increasing the deposition temperature. This results in a decrease in electric field, for example, through a factor of 1.8 between deposition temperatures of 48 and 60 K. Data in Figure 2 and Table 1 show

that, with increasing deposition temperature from 48 to 60 K, the LO mode redshifts from 2256.35 to 2255.4 cm^{-1}, whereas the TO mode blueshifts from 2239.15 to 2239.85 cm^{-1}. This suggests some sort of correlation between the LO-TO splitting and the spontelectric field, which we now set out to explore.

To make the connection between RAIRS results and the spontelectric effect, we first refer to a parameterized model for spontelectrics. This model successfully describes the variation with deposition temperature, of the observed spontelectric field in films of N_2O, of N_2O diluted in xenon7, of methyl formate and of CF_3Cl, CF_2Cl_2 and $CFCl_3$ films1.

A mean-field model is used to describe the spontelectric steady state. This model was originally introduced in [4] and is set out in detail in [1]. The model is based on the concept that the net z-component of the electric field within a spontelectric film and normal to the plane of the film, E_z, is composed of two parts. The first is a local symmetrical part, defining the interactions which both bind layers to one another and dictates the molecular force field and thus molecular vibrational frequencies. The second is an asymmetrical part, due to the long-range field which permeates the film. The symmetrical part is expressed as a constant term plus a dipole-dipole term, proportional to $(<\mu_z>/\mu)^2$, and representing average intermolecular dipole-dipole interactions. Here, $<\mu_z>/\mu$, the degree of dipole orientation, is the ratio of the average z-component of the dipole moment and the total dipole moment of the molecular species in the solid state, where the z-axis is perpendicular to the plane of the film. The $(<\mu_z>/\mu)^2$ form, adopted to describe dipole-dipole interactions, reflects the fact that all such interactions, involving dipole-image charge, extended dipoles and arrays of dipoles, follow this squared relation.[27,28,29] We note that the symmetrical part of the contribution to E_z is related to the 'local field' at any molecular site, as defined in standard texts.[30]

The asymmetrical part, $<E_{asym}><\mu_z>/\mu$, is equal to the observed spontelectric field and is found only in the description of spontelectrics, with no direct counterpart for any other form of material. This asymmetrical part resembles the Weiss field in ferromagnetism, which is assumed to be proportional to the magnetisation.[31] Here, read degree of dipole orientation for magnetisation and read polarisation field for the Weiss field. We emphasise that the polarisation field, that is, the spontelectric field, is self-generated within the spontelectric material. The polarization field acts in opposition to the symmetrical part and represents the long-range field created by the average dipoles and experienced by an average dipole.

Hence, using atomic units throughout,

$$E_z = \left\langle E_{sym} \right\rangle \left[1 + \zeta \left(\frac{\langle \mu_z \rangle}{\mu} \right)^2 \right] - \left\langle E_{asym} \right\rangle \frac{\langle \mu_z \rangle}{\mu}$$

(2)

where $<E_{sym}>$, $<E_{asym}>$ and ζ are taken to be temperature

independent parameters. The $\zeta(<\mu_z>/\mu)^2$ term in Equation (2) may be interpreted as a measure of the tendency of one dipolar species to restrict the angular motion of another, a 'locking' term or, as it is sometimes called, a 'frustration' term.

Mean field theory gives an implicit expression for $<\mu_z>/\mu$, yielding the familiar Langevin function for orientational interactions[30]

$$\frac{< \mu_z >}{\mu} = \coth \left(\frac{E_z \mu}{T} \right) - \left(\frac{E_z \mu}{T} \right)^{-1}$$

(3)

where T is the deposition temperature of the layer of material. The dipole moment of N_2O in the solid state is reduced from that in the gas phase through depolarization in the environment of other N_2O species according to:

$$\mu = \frac{\mu_0}{1 + \alpha k / s^3}$$

(4)

where s is the average spacing between successive layers, equal to 0.32 nm for N_2O,[1,4] α is the molecular polarizability of N_2O $(3.03 \times 10^{-30}$ m$^3)$, $k = 11.034$ [32] and μ_0 is the gas phase dipole moment of N_2O (= 0.166 D).

3.3. Contributions of the intrinsic effect and the Stark effect to the LO-TO splitting

The first three columns of Table 1 summarize RAIRS spectroscopic data, for LO-TO frequencies in solid N_2O, as a function of deposition temperature, T. These are shown as open symbols in Figure 4. Column 4 of Table 1 shows the LO-TO splitting, that is, column 3 – column 2. Column 5 shows the Stark splitting due to the spontelectric field, column 6 the ratio of this splitting compared to the total LO-TO splitting and the final column the degree of dipole orientation associated with each temperature of deposition, as derived from experimental data in [1].

The vibrational Stark effect, expressed as a frequency shift, is known to be linearly proportional to the perturbation provided by a local electric field8,[9,10,11]. Recollecting that the spontelectric field is given by the $<E_{asym}>$ multiplied by the degree of dipole orientation, we note that values in Table 1 show that the degree of dipole orientation, and therefore the spontelectric field, falls by a factor of ~4 between 48 and 66 K. However the LO-TO splitting, $\Delta\nu$, falls by a factor of ~1.3. We interpret this as demonstrating $\Delta\nu$ may be represented by the sum of two terms, one of which, the intrinsic splitting, $\Delta\nu_B$, is independent of temperature of deposition, whereas the other, $\Delta\nu_S$, the spontelectric term, is a function of temperature. Thus $\Delta\nu = \Delta\nu_S + \Delta\nu_B$. We can use the data in Table 1 to determine an experimentally based value of $\Delta\nu_B$. This gives the desired values of $\Delta\nu_S$, as a function of temperature.

T /K	TO /cm^{-1} ± 0.2	LO /cm^{-1} ± 0.1	$\Delta\nu$ /cm^{-1}	$\Delta\nu_S$ /cm^{-1}	$\Delta\nu_S/\Delta\nu$	$\langle\mu_z\rangle/\mu$
48	2239.15	2256.35	17.2	5.2	0.303	0.0813
51	2239.6	2255.9	16.3	4.3	0.265	0.0683
52	2239.8	2255.8	16.0	4.0	0.251	0.0639
53	2239.7	2255.8	16.1	4.1	0.256	0.0614
55	2240.05	2255.3	15.25	3.3	0.214	0.0565
56	2240	2255.3	15.3	3.3	0.217	0.0540
60	2239.85	2255.4	15.55	3.4	0.229	0.0449
62	2240.1	2254.9	14.8	2.8	0.191	0.0386
66	2240.8	2254.2	13.4	1.4	0.106	0.0117

Table 1: Measured frequencies, as shown in Figure 4, of the TO and LO modes in solid N$_2$O as a function of deposition temperature, T. $\Delta\nu$ is the measured LO-TO splitting and $\Delta\nu_S$ is that part due to the spontelectric field. The last column shows degree of dipole orientation associated with each deposition temperature.

This evaluation is performed as follows, noting that from hereon, the subscript L denotes the LO mode and T, the TO mode. Equally the subscript S refers to the spontelectric effect and B to the intrinsic effect. The Stark shift may be represented by $\phi_L.E_L$ for the LO frequency and $-\phi_T.E_T$ for the TO frequency, where ϕ_L and ϕ_T are the respective Stark tuning rates and E_L is the spontelectric field relevant to the LO mode and E_T for the TO mode. Therefore $\Delta\nu_S = \phi_L.E_L + \phi_T.E_T$ and $\Delta\nu_S(T_i)/\Delta\nu_S(T_j) = (\phi_L.E_L + \phi_T.E_T)_i/(\phi_L.E_L + \phi_T.E_T)_j$ where i and j refer to any two temperatures. We now introduce the simplifying *ansatz* that the Stark field tunes the LO and TO modes by quantities equal in magnitude but of opposite sign. This is supported by the experimental data in Table 1, which show that the average of ν_L and ν_T falls by only 0.3 cm^{-1}, from 2247.8 to 2247.5 cm^{-1}, over the full temperature range of 48 to 66 K, whereas $\Delta\nu$ falls by 3.8 cm^{-1}.

It follows from the above that values of $\Delta\nu_{Si}/\Delta\nu_{Sj}$ are equal to the ratios of degrees of dipole orientation at deposition temperatures T_i and T_j, where all values may be found in Table 1. The ratio of the total LO-TO splitting, $\Delta\nu_i/\Delta\nu_j$, is also given by values shown in Table 1. We may then write that

$$\frac{\Delta\nu_B}{\Delta\nu_{Sj}} = \frac{\left[\left(\langle\mu_z\rangle/\mu\right)_i\middle/\left(\langle\mu_z\rangle/\mu\right)_j - \Delta\nu_i/\Delta\nu_j\right]}{\left(\Delta\nu_i/\Delta\nu_j - 1\right)} \quad (5)$$

Now $\Delta\nu_j = \Delta\nu_B + \Delta\nu_{Sj}$ and substituting $\Delta\nu_{Sj}$ from Equation (5), we find $\Delta\nu_j = \Delta\nu_B(1+1/\psi)$ where ψ equals the rhs of Equation (5). Hence

$$\Delta\nu_B = \psi\Delta\nu_j/(1+\psi) \quad (6)$$

As a check on this analysis, values of $\Delta\nu_B$ derived from Equation (6) are found to be unchanged with deposition temperature, within experimental error. The average value is 12.0±0.35 cm^{-1}. The corresponding values of $\Delta\nu_S$, that is, those parts of the LO-TO splitting attributed to the spontelectric effect, are shown in Table 1. Within experimental error, these values are indeed

proportional to $\langle\mu_z\rangle/\mu$, which is itself proportional to the ambient spontelectric field at any deposition temperature. This is shown in Figure 6, which reflects the expected property that the vibrational Stark effect is linearly proportional to the perturbation provided by the local electric field.

The Stark tuning rate of the νNN transition may be estimated from the data in Figure 6 to be 2.9 cm^{-1} per MV cm^{-1} electric field, given that the linear fit goes through the origin. The extensive literature in the area of Stark vibrational tuning has been reviewed most recently in [33]. Data presented there, and elsewhere, reveal that Stark tuning rates tend to be 3 to 4 times lower than the figure that we propose here, with some exceptions involving higher rates. Remarks in [8] and [34] suggest that the presence of inherent dipole orientation in the sample, as proposed in the present work, may be the origin of an enhanced tuning rate in solid N$_2$O.

At all events, our contention is that the variation of $\Delta\nu_S$ with deposition temperature should follow that of the spontelectric field with deposition temperature, where the spontelectric field is given by $\langle E_{asym}\rangle(\langle\mu_z\rangle/\mu)$. We now address how to formulate the variation of this field with temperature.

3.4. A model for the temperature dependence of the LO and TO spectral features in spontelectric material based upon the vibrational Stark effect

3.4.1 Expressing the LO-TO splitting in terms of spontelectric parameters for N$_2$O.

The purpose of this section is to develop a model which shows how the spontelectric field may contribute to the observed value of the LO-TO splitting, relative to the TO frequency (say), through the vibrational Stark effect.

We have remarked above that the internal electronic structure of the individual molecules, influenced by electrostatic effects from neighbouring molecules, is responsible for TO modes. Thus $\langle E_{sym}\rangle[1+\zeta(\langle\mu_z\rangle/\mu)^2]$, the first term of Equation (2), may be regarded as the average effective electric field at any molecule, giving rise to the force field which determines the value of νNN in the TO mode. However, the occurrence of a spontelectric field adds an additional potential in the direction normal to the plane of the film, shifting the LO vibrations to yet higher wavenumber than in standard LO-TO splitting. Thus the force field for LO vibrations, as measured in RAIRS, includes an additional term involving the torque exerted on the molecular dipole in the spontelectric field. The field involved in this additional term has the form of the projection of the spontelectric field onto the direction in which the average dipole points, that is $\langle E_{asym}\rangle(\langle\mu_z\rangle/\mu)^2$. Dipole orientation also influences the force field dictating the TO mode, via the term $\langle E_{sym}\rangle\zeta(\langle\mu_z\rangle/\mu)^2$ in Equation (2) and the coupling of $\langle\mu_z\rangle/\mu$ to E_z in Equation (3).
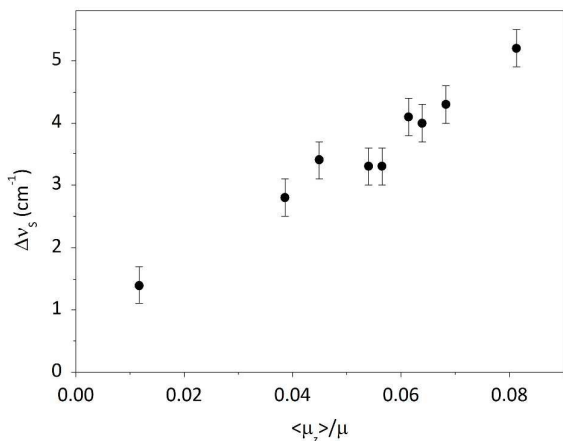
Figure 6. The variation of the part of the LO-TO splitting due to the spontelectric effect, $\Delta\nu_S$, in table 1, with $\langle\mu_z\rangle/\mu$, using values taken from Table 1.

Clearly the LO and TO modes possess two different effective force constants, reflecting the different force fields associated with LO and TO modes. Let k be the force constant associated with a fictitious solid, in the absence of either the spontelectric effect or effects leading to the intrinsic LO-TO splitting. Then in a real solid, two force constants may be encountered, k - δ_T and k + δ_L where, introducing the harmonic approximation, $\nu_L \propto$ (k + δ_L)$^{1/2}$ and $\nu_T \propto$ (k - δ_T)$^{1/2}$, recollecting that the LO frequency always lies higher than the TO frequency. We introduce the *ansatz* that $\delta_L = \delta_T = \delta$, which involves the assumption that the values of the parameters $\langle E_{sym}\rangle$, ζ and $\langle\mu_z\rangle/\mu$ are the same for both longitudinal and transverse modes. Given that $\delta \ll k$, then

$$\nu_L \propto \left[k\left(1+\delta/k\right)\right]^{1/2}/M^{1/2} \approx \left(k/M\right)^{1/2}\left(1+1/2\,\delta/k\right) \qquad (7)$$

and similarly for ν_T but with (1-½δ/k) on the rhs, where M is the molar mass of N_2O. Thus $\nu_L/\nu_T \sim (1+\frac{1}{2}\delta/k)^2 \sim 1 + \delta/k$, from which it follows that $\Delta\nu/\nu_T = \delta/k$, where $\Delta\nu = \nu_L - \nu_T$ as above. These approximations are accurate to better then ~0.4%, given that δ/k ~0.008 here.

We now let the energy, associated with the TO vibration, be U_T and that associated with the LO vibration be U_L. Again using $\delta \ll k$ and $\Delta\nu \ll \nu_T$ or ν_L, and the result just derived that $\Delta\nu/\nu_T = \delta$/k, it may readily be shown that

$$(U_L - U_T)/U_T = (\nu_T/\nu_L)[(1+\delta/k)/(1-\delta/k)] - 1 \qquad (8)$$

This then yields the following relationship between U_T and U_L and the observed LO-TO splitting:

$$(U_L - U_T)/U_T \sim \Delta\nu/\nu_T \qquad (9)$$

which is accurate to better than ~0.75% overall. In order to simplify the subsequent analysis, note that we have used $\Delta\nu/\nu_T \sim$ $\Delta\nu/\nu_L$ in writing Equation (9). Approximations involved in deriving Equation (9) lead to a negligible inaccuracy in the differential of $\Delta\nu/\nu_T$ with respect to $\langle\mu_z\rangle/\mu$, used in section 3.4.2.

We now set out to relate the ratio of U_L-U_T and U_T to parameters governing the spontelectric effect. Consider first the total field at the molecule, U_T, relevant to the TO mode. This total field includes that giving rise to both the intrinsic and spontelectric effects. Spontelectric effects may be represented by the term $\langle E_{sym}\rangle(1+\zeta(\langle\mu_z\rangle/\mu)^2)$, from Equation (2). Since the ratio of the total field to the spontelectric part $\propto \Delta\nu/\Delta\nu_S$, the total field governing ν_T must itself be proportional to $(\Delta\nu/\Delta\nu_S)\langle E_{sym}\rangle(1+\zeta(\langle\mu_z\rangle/\mu)^2)$. Second, U_L-U_T $\propto$ the spontelectric field times the degree of dipole orientation, giving the effective field. In each case there is an additional independent term describing the intrinsic LO-TO splitting, $\Delta\nu_B$. It then follows from Equation (9) that:

$$\frac{\Delta\nu}{\nu_T} \approx \frac{\left(\Delta\nu_S/\Delta\nu\right)\langle E_{asym}\rangle\left(\langle\mu_z\rangle/\mu\right)^2}{\langle E_{sym}\rangle\left[\left(1+\varsigma(\langle\mu_z\rangle/\mu)^2\right)\right]} + \frac{\Delta\nu_B}{\nu_T} \qquad (10)$$

Below, we use the theoretical model of spontelectrics, outlined in section 3.2, to establish an analytic expression for the variation of the degree of dipole orientation with deposition temperature. We then show that the LO-TO splitting and its variation with temperature follows the variation dictated by Equation (10). This is performed using appropriate values of the spontelectric parameters, $\langle E_{sym}\rangle$, ζ and $\langle\mu_z\rangle/\mu$, derived in section 3.4.3, obtained from fitting to experimental data presented in [1]. Further, a numerical check on Equation (10) is presented at the end of section 3.4.3, to establish self-consistency between values of $\Delta\nu_B$ derived from Equation (10), which is founded upon the Stark field interpretation and associated spontelectric theory of LO-TO splitting, and from Equation (6) which involves experimental quantities.

The differential of Equation (10) with respect to $\langle\mu_z\rangle/\mu$, multiplied by the differential of $\langle\mu_z\rangle/\mu$ wrt deposition temperature, gives the differential of the LO-TO splitting wrt temperature, the quantity which we seek. This is expressed here in terms of the variation of the individual LO and TO frequencies wrt T, using the quantities measured (Figure 4) and given in Table 1. The next task is to formulate the differential of the LO and TO frequencies wrt $\langle\mu_z\rangle/\mu$ in 3.4.2 and, following that, the differential of the LO and TO splitting wrt temperature of deposition, in 3.4.3.

3.4.2 Variation of the LO and TO frequencies with the degree of dipole orientation, $\langle\mu_z\rangle/\mu$.

It is our intention to differentiate Equation (10) wrt the degree of dipole orientation, $\langle\mu_z\rangle/\mu$. We choose here to make the approximation that the intrinsic effect, expressed as $\Delta\nu_B$, is independent of $\langle\mu_z\rangle/\mu$. In doing so we recognise that $\Delta\nu_B$ may in

principle be affected by the degree of dipole alignment, since the potentials associated with transverse and longitudinal motions will be influenced by dipole alignment. If these potentials are affected each in a different manner, the intrinsic effect will have a temperature dependence due to the temperature dependence of the spontelectric effect. Thus the intrinsic and spontelectric effects may be coupled together. For simplicity however, we make the assumption that any such coupling may be ignored.

The data in Figure 4 show that the average rate of change of ν_L with deposition temperature, taken over the temperature range 48 to 60 K is -0.1 ± 0.020 cm^{-1} K^{-1} and of ν_T is 0.06 ± 0.022 cm^{-1} K^{-1}. The simplifying assumption is now made that these rates are indistinguishable numerically, since they overlap within experimental error. We note that there is no fundamental reason why the absolute values of these rates should be equal; it is just a convenience in the present case of N_2O. For CO, for example, this does not hold (work in preparation). At all events, $d\nu_L/dT|_T = -d\nu_T/dT|_T$ implies $d\nu_L/d{<}\mu_z{>}/\mu|_T = -d\nu_T/d{<}\mu_z{>}/\mu|_T$.

Following some manipulation, we find

$$\frac{d\nu_T}{d\langle\mu_z\rangle/\mu} = -\frac{\langle E_{sym}\rangle\langle E_{asym}\rangle(\langle\mu_z\rangle/\mu)(\nu_L - \Delta\nu_B)\{2\xi + (\langle\mu_z\rangle/\mu)\eta\xi'\}}{\{\langle E_{sym}\rangle\eta + \langle E_{asym}\rangle(\langle\mu_z\rangle/\mu)^2\xi]\}\{2\langle E_{sym}\rangle\eta + \langle E_{asym}\rangle(\langle\mu_z\rangle/\mu)^2\xi]\}} \quad (11)$$

where $\xi = \Delta\nu_S/\Delta\nu$, $\eta = {<}E_{sym}{>}(1+\zeta({<}\mu_z{>}/\mu)^2)$ and $\xi' = d(\Delta\nu_S/\Delta\nu)/d{<}\mu_z{>}/\mu$ or $(\Delta\nu_B/\Delta\nu^2)$ $d(\Delta\nu_S)/d{<}\mu_z{>}/\mu$. In evaluating Equation (11), we introduce an empirical value of $\xi' = d(\Delta\nu_S/\Delta\nu)/d({<}\mu_z{>}/\mu) = 51.6\ {<}\mu_z{>}/\mu - 0.631$, a relation obtained using values in Table 1.

Note that Equation (11) shows an increase in ν_T as ${<}\mu_z{>}/\mu$ decreases, that is, an increase in the transverse optical frequency as the temperature of deposition rises – or the reverse for the longitudinal optical frequency. This follows the experimental behaviour shown in Figure 4.

3.4.3 Variation of the LO and TO frequencies with the temperature of deposition

We now require an expression for $d({<}\mu_z{>}/\mu)/dT$. On evaluation, this can then be multiplied by Equation (11) to yield the desired expressions for $d\nu_T/dT$ and $d\nu_L/dT$ vs T. These expressions may then, on integration, be compared with the experimental data in Table 1 for the variation of $\Delta\nu$ with temperature of deposition.

An expression for $d({<}\mu_z{>}/\mu)/dT$ has in fact been presented elsewhere[1] but for completeness it is given again here. Substituting Equation (2) for E_z (in Section 3.2) into Equation (3) for ${<}\mu_z{>}/\mu$ and differentiating the result wrt T, the temperature of deposition, gives:

$$\frac{d{<}\mu_z/\mu{>}}{dT} = \frac{1/\mu E_z - (\mu E_z/T^2)\cos ech^2(\mu E_z/T)}{(\mu E'/T)\cos ech^2(\mu E_z/T) - E'T/\mu E_z^2 - 1} \quad (12)$$

where $E' = {<}E_{asym}{>} - 2\varsigma {<}E_{sym}{>}{<}\mu_z/\mu{>}$. Multiplying Equation (11) by Equation (12) yields $d\nu_T/dT$ ($= - d\nu_L/dT$). We now seek to compare the numerical values of the product of Equations 11 and 12 with experimental data.

We need first however to establish appropriate values of the spontelectric parameters ${<}E_{sym}{>}$, ${<}E_{asym}{>}$ and ζ. These are required to fit experimental data for the spontelectric field and the degree of dipole orientation between 48 and 62 K. In this connection, we note that the spontelectric model cannot reproduce the downturn in dipole orientation or spontelectric field, observed closer to the sublimation temperature at ~66 K.[1] For this reason we ignore data at 66 K from hereon.

Using a single set of spontelectric parameters, the model set out in [1], summarised in section 3.2, fits data accurately between 38 and 48 K but departs from agreement at > 48 K. Our RAIRS data indicate that this is due to a phase change in solid N_2O at ~48 K, from one spontelectric phase to another. This is demonstrated by both the abrupt change, described in section 2, in the RAIRS linewidth at this temperature and the departure, just mentioned, between model and experiment at > 48 K. Moreover, neutron scattering data and Temperature-Programmed Desorption experiments, reported elsewhere (in prepartion), show clear evidence of a structural change around 48 K.

Such a phase change around 48 K flags a change in the potential landscape and implies a requirement for new values of the spontelectric parameters ${<}E_{sym}{>}$, ${<}E_{asym}{>}$ and ζ. To fit data for the observed spontelectric fields at ≥ 48 K in [1], we find ${<}E_{sym}{>}$ = 4.57×10^8 V m^{-1} (reduced from 5.43×10^8 V m^{-1} in [1]), ${<}E_{asym}{>}$ = 8.63×10^8 V m^{-1} (increased from 7.88×10^8 V m^{-1}) and $\zeta = 75$ (increased from 43.8), values which fit experimental data for electric fields in the sample, and values of ${<}\mu_z{>}/\mu$ deduced from those electric fields, vs deposition temperature for ≥ 48 to 60 K to better than 3%, save for 60 and 62 K data where the error approaches 10 to 15%. Note the current modification of spontelectric parameters leads to some small modifications in the values of ${<}\mu_z{>}/\mu$ reported here (Table 1), compared with values given in [1].

These modified spontelectric parameters are now used to evaluate Equations (11) and (12). Table 2 shows the results of such calculations and their product, that is, the values of $d\nu_T/dT$. Note that the figures shown in Table 2 are in each case local to the temperature, or degree of dipole orientation, at which they are evaluated.

In addition, the internal consistency of Equation (10) may now be checked, given the values of ${<}E_{sym}{>}$ = 4.57×10^8 V m^{-1}, ${<}E_{asym}{>}$ = 8.63×10^8 V m^{-1} and $\zeta = 75$ established above. Rearranging

Equation (10), the value of the intrinsic term, $\Delta\nu_B$, averaged over 48 to 56 K is found to be 12.5 ± 0.3 cm^{-1}, using values for $\Delta\nu_S/\Delta\nu$, $\Delta\nu$, ν_T and $<\mu_z>/\mu$ taken from Table 1. For comparison, the value of $\Delta\nu_B$ from Equation (6), independent of the spontelectric parameters mentioned, gave 12.0 ± 0.35 cm^{-1}. These two values are in agreement within experimental error.

T /K	$-d\nu_T/d<\mu_z>/\mu$ /cm^{-1}	$-d<\mu_z>/\mu/dT$ /K	$d\nu_T/dT$ /cm^{-1} K^{-1}	Model $\Delta\nu$ /cm^{-1}	Observed $\Delta\nu$ /cm^{-1}
48	76.9	0.00430	0.330	17.8	17.2
51	65.8	0.00253	0.167	16.4	16.3
52	61.3	0.00218	0.129	16.1	16.0
53	60.6	0.00197	0.119	15.8	16.1
55	51.0	0.00164	0.0836	15.4	15.25
56	49.8	0.00150	0.0748	15.3	15.3
60	44.9	0.00111	0.0446	14.75	15.55
62	34.2	0.00183	0.0625	14.6	14.8

Table 2: Column 1: temperature of deposition, T. Column 2: calculated values of the rate of change of ν_T with degree of dipole orientation (Equation (11)). Column 3: Calculated values of the rate of dipole orientation with temperature of deposition (Equation (12)). Column 4: Calculated values of the rate of change of ν_T, the TO frequency, with temperature of deposition. Column 5: values of the LO-TO splitting estimated from the model. Column 6: experimental values for comparison

3.5. Comparison between experiment and model

Our goal was to compare the variation of LO-TO splitting with deposition temperature to the properties of spontelectrics. This comparison is now performed using values of the LO-TO splitting, $\Delta\nu$ in Table 1, and those estimated from the analysis presented in subsections of 3.4.

We use values of $d\nu_T/dT$ from Table 2, recollecting that $d\nu_T/dT = -d\nu_L/dT$. A third order polynomial in the temperature of deposition may be accurately drawn through these values of the derivative. This polynomial is integrated to give an expression for ν_T and ν_L vs temperature of deposition, which is then fourth order in this temperature. In each case a constant of integration, k_T and k_L respectively, may be determined using the measured values of ν_T and ν_L, in Table 1. $\Delta\nu$ is then given by $(k_L - k_T)$ less twice the value of the 4th order polynomial at the relevant temperature. This constructs the desired variation of $\Delta\nu$ with T, according to the model, without any further parametrization or adjustment.

The result of this procedure is shown as a solid line in Figure 7. Numerical uncertainties in $\Delta\nu$ of ~±0.8 cm^{-1} may be assigned to values extracted from the model, estimated from the error inherent in the constants of integration, k_L and k_T, and in the value of ξ' in Equation (13). Thus the solid line in Figure 7 may be shifted up or down by 0.8 cm^{-1}. Given this, experimental and model values of variation of the LO-TO splitting with deposition temperature agree satisfactorily. There appears however to be

some discrepancy at 60 K.
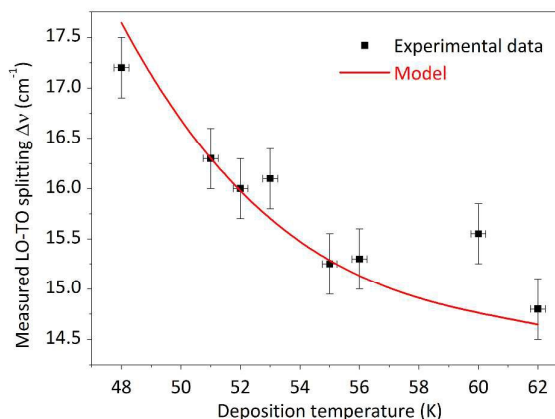
Figure 7: Comparison between model and experiment. Points represent the experimental variation of the LO-TO splitting, $\Delta\nu$, vs temperature of deposition, using values given in Table 1. Errors of ±0.3 cm^{-1} have been assigned to values of $\Delta\nu$, in accord with individual errors of ±0.1 and ±0.2 cm^{-1} for LO and TO frequencies, respectively. The solid line represents the variation of $\Delta\nu$ based upon the spontelectric model presented in the text. For numerical uncertainties in the model, see text.

4. Concluding remarks

The significance of the results in section 3 is as follows. Our analysis is based squarely upon the occurrence of the spontelectric effect in N$_2$O films. This analysis can be used to reproduce both qualitative and quantitative features of the LO-TO splitting and its variation with deposition temperature of N$_2$O films. This therefore gives considerable credence to the contention that the data presented here are independent evidence for the presence of a powerful electric field within the solid film and thus for the occurrence of the spontelectric effect. Further, since our analysis is founded on the premise that the spontelectric effect has a basis in dipole orientation, the current results provide further support for this model of the effect.

In addition we have shown here that the magnitude of the LO-TO splitting in solid state spectroscopy of N$_2$O has a significant contribution from the spontelectric effect. This contribution, given by $\Delta\nu_S/\Delta\nu$ in Table 1, extends from 30% at 48 K to 10% at 66 K. This must be a general phenomenon and introduces a new factor in our understanding of LO-TO splitting in molecular films when these are known to be spontelectric, in particular with regard to any anomalously large temperature dependence of LO-TO splitting. We suggest therefore that any such anomalous temperature dependence is good evidence that the solid film is spontelectric.

5

Notes and References

[1] D. Field, O. Plekan, A. Cassidy, R. Balog, N. C. Jones, and J. Dunger, *Int. Rev. Phys. Chem.*, 2013, **32**, 345

[2] R. Balog, P. Cicman, N. Jones, and D. Field, *Phys. Rev. Lett.*, 2009, **102**, 2

[3] D. Field, O. Plekan, A. Cassidy, R. Balog, and N. Jones, *Europhys. News*, 2011, **42**, 32

[4] O. Plekan, A. Cassidy, R. Balog, N. C. Jones, and D. Field, *Phys. Chem. Chem. Phys.*, 2011, **13**, 21035

[5] O. Plekan, A. Cassidy, R. Balog, N. C. Jones, and D. Field, *Phys. Chem. Chem. Phys.*, 2012, **14**, 9972

[6] A. Cassidy, O. Plekan, R. Balog, N. C. Jones, and D. Field, *Phys. Chem. Chem. Phys.*, 2012, **15**, 108

[7] A. Cassidy, O. Plekan, , J.Dunger, R. Balog, N. C. Jones, J. Lasne, A.Rosu-Finsen, M.R.S.McCoustra and D. Field, *Phys. Chem. Chem. Phys.*, 2014, **16**, 23843

[8] S.A. Andrews, S.G.Boxer, *J. Phys. Chem. A*, 2002, **106**, 469

[9] E. S. Park, S. G. Boxer, *J. Phys. Chem. B*, 2002, **106**, 5800

[10] I.T. Suydam, S.G.Boxer, *Biochemistry*, 2003, **42**, 12050

[11] G. Schkolnik, J. Salewski, D. Millo, I. Zebger, S. Franzen, P. Hildebrandt, *Int. J. Mol. Sci.*, 2012, **13**, 7466

[12] D. Berreman, *Phys. Rev.*, 1963, **130**, 2193

[13] L.H. Jones, B.I. Swanson, *J. Phys. Chem.*, 1991, **95**, 2701

[14] M. A. Ovchinnikov, C. A. Wight, *J. Chem. Phys.*,1993, **99**, 3374

[15] M. A. Ovchinnikov, C. A. Wight, *J. Chem. Phys.*,1994, **100**, 972

[16] S.A. Andrews, S.G.Boxer, *J. Phys. Chem. A*, 2002, **106**, 469

[17] E. S. Park, S. G. Boxer, *J. Phys. Chem. B*, 2002, **106**, 5800

[18] I.T. Suydam, S.G.Boxer, *Biochemistry*, 2003, **42**, 12050

[19] G. Schkolnik, J. Salewski, D. Millo, I. Zebger, S. Franzen, P. Hildebrandt, *Int. J. Mol. Sci.*, 2012, **13**, 7466

[20] H. J. Fraser, M. P. Collings, and M. R. S. McCoustra, *Rev. Sci. Instrum.*, 2002, **73**, 2161

[21] V.L. Frankland, A. Rosu-Finsen, J. Lasne, M.P. Collings and M.R.S. McCoustra, *Rev. Sci. Instrum.*, 2015, **86**, 055103

[22] J.D. Thrower, M.P. Collings, F.J.M. Rutten and M.R.S. McCoustra, *Mon. Not. R. Astron. Soc.*, 2009, **394,** 1510

[23] J.E. Bartmess and R.M. Georgiadis, *Vacuum*, 1983, **33**, 149

[24] D. Fulvio, B. Sivaraman, G.A. Baratta, M.E. Palumbo and N.J. Mason, *Spectrochim. Acta Part A*, 2009, **72**, 1007

[25] A. Lapinski, J. Spanget-Larsen, J. Waluk and J.G. Radziszewski, *J. Chem. Phys.*, 2001, **115**, 1757

[26] E. Garrone, P. Ugliengo, G. Ghiotti, E. Borello and V.R. Saunders, *Spectrochim. Acta*, 1993, **49A**, 1221

[27] E. Cohen de Lara and J. Vincent-Geisse, *J. Phys. Chem.*, 1976, **80**, 1922

[28] B. L. Maschhoff and J. P. Cowin, *J. Chem. Phys.*, 1994, **101**, 8138

[29] D. Fernández-Torre, O. Kupiainen, P. Pyykkö, and L. Halonen, *Chem. Phys. Lett.*, 2009, **471**, 239

[30] C. Kittel, *Introduction to Solid StatePhysics*, Wiley, 3rd edition., 2005

[31] H. Kliem, M. Kuehn, and B. Martin, *Ferroelectrics*, 2010, **400**, 41

[32] J.Topping, *Proc. R. Soc. London Ser. A.,* 1927, **114**, 67

[33] S. Fried, S. G. Boxer, *Acc. Chem. Res.*, 2015, 48, 998

[34] N. M. Levinson, S. D. Fried, S. G. Boxer, *J. Phys. Chem. B*, 2012, **116**, 10470